### Title
Subchronic co-exposure to particulate matter and fructose-rich-diet induces insulin resistance in male Sprague Dawley rats




### Authors
Jiménez-Chávez, Arturo
Morales-Rubio, Russell
Sánchez-Gasca, Eliu
et al.



### Publication Date
2023-06-01

### DOI
10.1016/j.etap.2023.104115

Peer reviewed

Environmental Toxicology and Pharmacology 100 (2023) 104115

Contents lists available at ScienceDirect

Environmental Toxicology and Pharmacology

journal homepage: www.elsevier.com/locate/etap

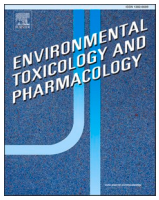

# Subchronic co-exposure to particulate matter and fructose-rich-diet induces insulin resistance in male Sprague Dawley rats

Arturo Jiménez-Chávez [a], Russell Morales-Rubio [a], Eliu Sánchez-Gasca [a], Mónica Rivera-Rosas [a], Marisela Uribe-Ramírez [a], Omar Amador-Muñoz [b], Y. Margarita Martínez-Domínguez [b], Irma Rosas-Pérez [b], Elizabeth H. Choy [c], David A. Herman [c], Michael T. Kleinman [c], Andrea De Vizcaya-Ruiz [a,c,*,1]

[a] Departamento de Toxicología, Centro de Investigación y de Estudios Avanzados del IPN (CINVESTAV-IPN), Ciudad de México, México
[b] Instituto de Ciencias de la Atmósfera y Cambio Climático, Universidad Nacional Autónoma de México, Ciudad Universitaria, Ciudad de México, México
[c] Department of Environmental and Occupational Health, Program in Public Health, Susan and Henry Samueli College of Health Sciences, University of California Irvine, Irvine, CA, USA

ARTICLE INFO

Edited by Dr. Malcolm D. Tingle

*Keywords:*
Particulate matter
Fructose rich diet
Hyperinsulinemia
Insulin resistance
Insulin/AKT pathway

ABSTRACT

Insulin resistance (IR) and metabolic disorders are non-pulmonary adverse effects induced by fine particulate matter ($PM_{2.5}$) exposure. The worldwide pandemic of high fructose sweeteners and fat rich modern diets, also contribute to IR development. We investigated some of the underlying effects of IR, altered biochemical insulin action and Insulin/AKT pathway biomarkers. Male Sprague Dawley rats were subchronically exposed to filtered air, $PM_{2.5}$, a fructose rich diet (FRD), or $PM_{2.5}$ + FRD. Exposure to $PM_{2.5}$ or FRD alone did not induce metabolic changes. However, $PM_{2.5}$ + FRD induced leptin release, systemic hyperinsulinemia, and Insulin/AKT dysregulation in insulin-sensitive tissues preceded by altered $AT_1R$ levels. Histological damage and increased HOMA-IR were also observed from $PM_{2.5}$ + FRD co-exposure. Our results indicate that the concomitant exposure to a ubiquitous environmental pollutant, such as $PM_{2.5}$, and a metabolic disease risk factor, a FRD, can contribute to the metabolic disorder pandemic occurring in highly polluted locations.

## 1. Introduction

Airborne particulate matter (PM) is a ubiquitous environmental pollutant that impacts most of the global population. As of 2019, the World Health Organization (WHO) estimates that 99% of the world's population lives in areas that did not meet current air quality standards ("WHO, ", 2022). Exposure to ambient PM with an aerodynamic diameter of 2.5 μm or less ($PM_{2.5}$) has been associated with metabolic non-communicable diseases like obesity, metabolic syndrome or diabetes (Cervantes-Martínez et al., 2022; Chilian-Herrera et al., 2021; Zhang et al., 2021). The oxidative and pro-inflammatory response induced from $PM_{2.5}$ exposure have also been suggested as underlying mechanisms of metabolic diseases; including dyslipidemia and numerous insulin-involved pathways (Xu et al., 2012; Xu et al., 2019).

An important and underappreciated factor in modern diets is the prevalence of the use of high fructose sweeteners. Consumption of these sweeteners increased > 1000% between 1970 and 1990 in the U.S. (Bray and Popkin, 2004). High level of consumption of these sweeteners can induce endocrine and metabolic effects that contribute to metabolic syndrome and obesity (Stanhope and Havel, 2008; Lancaster, 2020).

Insulin resistance (IR) is defined as the impaired insulin action on tissues/organs and is considered a predictor process of metabolic disease development (Collares-Buzato, 2016). IR is characterized by impaired fasting glucose levels, increased blood insulin levels, augmented levels of lipid synthesis and pro-inflammatory markers, and molecular signaling alterations of the insulin pathway in insulin-sensitive tissues (i.e., liver, skeletal muscle, white adipose tissue) (Brierley and Semple, 2021). Moreover, the quotient between fasting glucose and insulin concentration, the homeostasis model assessment of insulin resistance (HOMA-IR), is a commonly used clinical standard (Freeman and

* Correspondence to: Avenida Instituto Politécnico Nacional No. 2508. Col. San Pedro Zacatenco, México D.F. C.P. 07360, Mexico.
*E-mail addresses:* adevizca@uci.edu, avizcaya@cinvestav.mx (A. De Vizcaya-Ruiz).
[1] Department of Environmental and Occupational Health, Program in Public Health, Susan and Henry Samueli College of Health Sciences, University of California Irvine, Irvine, CA, 92697, USA

https://doi.org/10.1016/j.etap.2023.104115
Received 21 November 2022; Received in revised form 19 March 2023; Accepted 29 March 2023
Available online 17 April 2023

Pennings, 2022; Peterson and Shulman, 2018). The homeostasis model assessment of β-cell function (HOMA-β) is another clinical standard and is used as an index of insulin secretory function derived from fasting plasma glucose and insulin concentrations (Matthews et al., 1985). However, both indexes cannot stand alone as sole criterion for metabolic disease prediction, and thus need of support of adjunct biomarkers.

Insulin can activate the protein kinase B (PKB/AKT) pathway which initiates the phosphorylation-dependent interaction between the insulin receptor and the insulin receptor substrate (IRS), phosphoinositide 3-kinase (PI3K), and protein kinase B (AKT). The activation of these proteins leads to down-stream events like glucose transport and uptake, glycogen synthesis, or lipid synthesis (Boucher et al., 2014). The systemic increase of insulin throughout the IR process can increase activation of the insulin/AKT pathway and lead to the imbalance of metabolic functions, such as glucose transport and lipid synthesis, in various tissues (Huang et al., 2018).

Diet is known to be a critical factor in the pathogenesis of IR and metabolic diseases. Western diets mainly consist of carbohydrates (~50%), fat (~30%) and proteins (~20%) (Mietelska-Porowska et al., 2022). The Western diet can promote metabolic changes like hyperinsulinemia and IR; in addition to increasing concentrations of reactive oxygen species (ROS) and oxidative stress (OxS); low-grade inflammation; and abnormal function of regulatory hormonal systems such as the renin-angiotensin system (RAS) (Kopp, 2019). Conversely, the fructose rich diet (FRD) model in animals can promote *de novo* lipogenesis and increase the synthesis of uric acid and inflammatory markers which lead to tissue specific damage (liver, skeletal muscle, hearth, blood vessels) and insulin resistance induction (Wong and Brown, 2014).

We have previously reported induction of OxS (Nrf-2 translocation, and increase of antioxidant response elements: super oxide dismutase 2 and hemeoxygenase 1 protein expression), inflammatory response (IL-1β, IL-6, MIP-2 in lung tissue); and activation of the RAS (increased blood pressure; angiotensin converter enzyme and angiotensin II type 1 receptor $AT_1R$ protein expression modification) in lung, heart and kidney of Sprague Dawley rats exposed to $PM_{2.5}$ (Aztatzi-Aguilar et al., 2015; Aztatzi-Aguilar et al., 2016; Aztatzi-Aguilar et al., 2018). Increases in HOMA-IR and HOMA-β, clinical hallmarks of IR, fasting glucose, in addition to fasting insulin and blood leptin levels have been associated with the increase in annual average ambient $PM_{2.5}$ concentrations (Wolf et al., 2016; Zhang et al., 2021). Furthermore, recent studies have reported the disruption in metabolism and transport from lipids and glucose, and the modification of metabolic pathways following $PM_{2.5}$ exposure (Haberzettl et al., 2016; Hill et al., 2021). However, the underlying mechanisms that participate in IR have not been fully investigated and much less in relation with an "energy-rich" diet. In this study, we determined that co-exposure to ambient $PM_{2.5}$ and a FRD could generate an insulin resistance state that leads to an Insulin/AKT pathway disruption and pathophysiological damage to insulin-sensitive tissues (i.e., liver, skeletal muscle, white adipose tissue) in male Sprague Dawley rats.

## 2. Materials and methods

### 2.1. Animals and exposure experimental design

Sprague Dawley rats (male, 8 weeks old) were obtained from the Laboratory Animal Production and Experimentation Unit [UPEAL in Spanish - *Unidad de Producción y Experimentación de Animales de Laboratorio*] at Cinvestav IPN. Animal care and experimental procedures were performed under the guideline NOM-062 ZOO-1999 in compliance with Mexican law and in accordance with the "Principles of Laboratory Animal Care" guidelines and approved by the Internal Committee for the Use and Care of Laboratory Animals (CICUAL in Spanish – *Comité Interno para el Cuidado y Uso de los Animales de Laboratorio*) under protocol No. 0312–20. Animals were housed at the animal facility at Cinvestav according to institutional guidelines and kept on a 12/12 light/dark cycle with food and water available ad libitum; relative humidity in the vivaria remained between 40% and 60% with a temperature range from 20 °C to 23 °C. Rats were randomly divided in 4 groups (n = 8/group). Each group was subchronically (8 weeks) exposed to filtered air (FA), concentrated ambient $PM_{2.5}$ ($PM_{2.5}$), filtered air plus fructose rich diet (FRD), or co-exposed to concentrated ambient $PM_{2.5}$ plus FRD ($PM_{2.5}$ + FRD) (Fig. 1).

#### 2.1.1. $PM_{2.5}$ exposure model

The present study was carried out in the North of Mexico City in an industrial area with high vehicular flow (De Vizcaya-Ruiz et al., 2006). Concentrated ambient $PM_{2.5}$ was generated using a versatile aerosol concentration enrichment system (VACES) located within the Experimental Laboratory of Inhalation Toxicology at the Animal Care Unit at Cinvestav IPN. The VACES has been routinely used for animal exposures in real-world environments and is able to concentrate ambient particles (0.02–10 μg) up to a factor of 10 (Herman et al., 2020; Kleinman et al., 2007; Kim et al., 2001). During exposures, the rats were confined in previously validated whole-body chambers (Oldham et al., 2004) and breathed either filtered air (FA) or concentrated ambient $PM_{2.5}$ ($PM_{2.5}$) atmospheres for 5 h/day, 4 days/week, for 8 weeks (October to December 2020) (Fig. 1).

Particle concentrations of both FA and $PM_{2.5}$ atmospheres as well as in the ambient environment were monitored throughout the exposure period using a condensation particle counter (Model 3787, TSI, Shoreview, MN). To analyze the major elements contained in particles. $PM_{2.5}$ samples from the exposure chambers were collected on polytetrafluoroethylene (PTFE) membrane filters (47 mm in diameter with 2 μm pore size; GE healthcare, Amersham Place, UK). The filters were acclimated and weighed in a temperature- and humidity-controlled facility before and after sampling. The calculated particle mass was used to derive particle dose delivered to the animals.

#### 2.1.2. Fructose rich diet (FRD) model

As mentioned before, consumption of a fructose rich diet or FRD has been associated with lipid synthesis and inflammatory modulation leading to specific tissue damage (liver, skeletal muscle, white adipose tissue (WAT)) and IR. To investigate if a FRD contributes to the adverse response to $PM_{2.5}$ exposure, we challenged two group of rats with a fructose rich diet ad libitum (via 20% fructose water solution) and exposed them to $PM_{2.5}$ or filtered air for 8 weeks.

#### 2.1.3. Tissue collection

At the end of the 8-week exposure period (and after 24 h the last

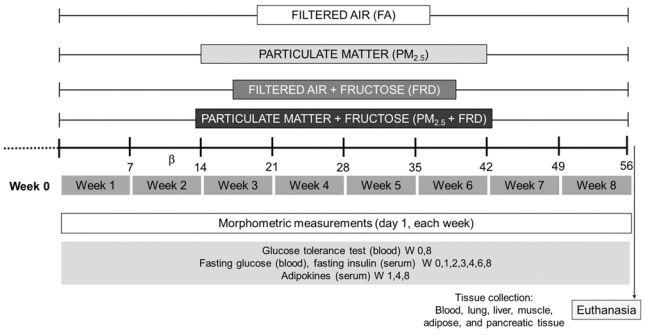


**Fig. 1. Experimental design.** In day 1 from the experimental design, the corresponding FRD groups started with the fructose in water. Since the day 2 to day 5, from each week, group animals were exposed to filtered air (FA) or $PM_{2.5}$ for 5 h. At the first day from each week, the anthropometric measures from 4 animal groups (n = 8) were determined. In several weeks during the subchronical exposure blood samples were obtained to determine different blood parameters. At the day 56, the last day of exposure, animals were euthanized, and several tissues were collected for their analysis.

exposure), the animals were anesthetized and euthanized by exsanguination. Lung, blood, liver, skeletal muscle (posterior limb), pancreas and visceral white adipose tissue (WAT) from 6 animals per group were dissected, snap-frozen in liquid nitrogen and stored at – 70 ºC until analysis. For histological analysis, the liver, muscle, pancreatic and adipose tissue from 2 animals per group were fixed in 10% phosphate-buffered formaldehyde, embedded in paraffin, and stained with hematoxylin/eosin for visualization. Glucose tolerance test (GT) blood samples were collected from the lateral tail vein for fasting glucose and fasting insulin levels.

### 2.2. $PM_{2.5}$ chemical composition determination

Organic compounds were determined using gas chromatography–mass spectrometry (GC-MS). Briefly, organic compounds, mainly polycyclic aromatic hydrocarbons (PAHs), were extracted from $PM_{2.5}$ by ultrasound-assisted extraction using ethanol as extraction solvent and analyzed via gas chromatograph-mass spectrometer equipped with a quadrupole mass filter and autosampler model 7683 (GC–qMS) (model 6890 plus/5973 N, Agilent Technologies, Santa Clara, CA, USA) (Beristain-Montiel et al., 2016). Analyses for major elements (Li, B, V, Cr, Co, Cu, As, Sr, Mo, Cd, Cs, Ba, Hg, Bi, Sn, Sb, Al, Se, Pb, Ni, Tl, Mn, Fe and Zn) were performed using ICP-MS (Thermo Fisher Scientific, Bremen, Germany). In brief, particle-loaded filters were sonicated in methanol for two minutes and the resulting particle suspension was dried under nitrogen. Dry particles were then resuspended in double deionized acidified water ($HNO_3$ 65% water diluted until a 0.16% final acid concentration was achieved) and sonicated for a homogeneous suspension for final ICP-MS analysis. A multi-element calibration standards™ 2, 3, 4, and 5 (Perkin Elmer, Waltham, MA, USA) was used to identify and quantify the elemental composition of $PM_{2.5}$ (Montes-Castro et al., 2019).

### 2.3. $PM_{2.5}$ endotoxin measurement

The concentration of endotoxin within the $PM_{2.5}$ samples was quantified using a Pyrochrome, Kinetic Chromogenic assay (Chromogenic Endotoxin Quant Kit A39552, Pierce ThermoFisher Scientific, Waltham, MA). $PM_{2.5}$ dispersions were prepared at 1 mg/mL in endotoxin free water. Absorbance measurements were obtained at 405 nm wavelength using a Pyros Kinetix Flex Instrument (Associates of Cape Cod, Inc.) as described in Falcon-Rodriguez et al. (2017).

### 2.4. Cytokine quantification

The serum adipokines and cytokines including interleukin 1β (IL-1β), tumor necrosis factor α (TNF-α), monocyte chemoattractant protein 1 (MCP-1), plasminogen activator inhibitor type 1 (PAI-1) and leptin were measured in serum at 1, 4 and 8 weeks of exposure using a RADPCMAG-82 K MILLIPLEX ® MAP Rat Adipocyte panel (EMD Millipore, Billerica, MA, USA).

### 2.5. Glucose tolerance test, fasting glucose, and insulin levels detection

Glucose tolerance (GT) was determined during week 0 and 8. For this test, rats were fasted for 8 h and underwent an assessment of fasting glucose levels time 0. Glucose (2 mg/g body weight) was then administrated by gavage, and GT was determined at 15, 30, 60 and 120 min after glucose administration (Glucocard™ test strips; ARKRAY Factory Inc., Netherlands). Fasting glucose levels were determined at weeks 0, 1, 2, 3, 4, 6, and 8 using the Glucocard™ test strips (ARKRAY Factory Inc., Netherlands) following an 8-hour fasting. Serum insulin levels were determined using EZRMI-13 Rat/ Mouse ELISA (EMD Millipore, Billerica, MA, USA) kit.

Based on the equivalence from 1 mg of insulin = 24 international units (IU), the homeostatic model assessment of insulin resistance index (HOMA-IR) was calculated according to the formula HOMA-IR = [fasting insulin concentration (ng/mL) × fasting glucose concentration (mg/dL) × 24]/405. The homeostatic model assessment of β-cells function (HOMA-β) was calculated by the formula HOMA-β = [360 × fasting insulin concentration (ng/mL)] / [fasting glucose concentration (mg/dL) – 63] (Li et al., 2020; Liu et al., 2014).

### 2.6. Western blot (WB) analysis

Western blots were performed according to protocols outlined in Burnette (1981) and MacPhee (2010). Briefly, frozen tissues (lung, liver, muscle, and adipose tissue) were homogenized in a nonionic, non-denaturing detergent (Nonidep-P40, Sigma Aldrich) with protease and phosphatase inhibitors and centrifuged at 14,000 rpm at 4 ºC. The supernatant was collected, and protein concentration was determined by the Bradford protein assay (Kruger, 1996). Subsequently, 30 μg of protein was electrophoresed (SDS-PAGE) and transferred to nitrocellulose membranes and blocked for 2 h with 5% of non-fat milk in Tris Buffer Solution (TBS). Membranes were incubated overnight with one of the proteins listed in Table 1 Supplementary information. Actin (1:1000 mouse monoclonal antibody; sc-8432, Santa Cruz Biotechnology, Tx, USA) was used as a loading control. Horseradish peroxidase (HRP)-conjugated secondary antibody (1:10000; Bio-Rad Laboratories, Hercules, CA, USA) was incubated with the membranes at room temperature for 1 h. HRP expression were subsequently detected using the Luminata Forte Western HRP substrate reagent (Millipore, Burlington, MA, USA). The expression levels were visualized by exposure to X-ray film and quantified by optical densitometry using ImageJ software (ImageJ, U. S. National Institutes of Health, Bethesda, Maryland, USA).

### 2.7. Histological analysis

Tissues embedded in paraffin (liver, skeletal muscle, WAT and pancreas) from the 4 exposure groups were sectioned at 5 μm, mounted, and stained with Hematoxylin/Eosin (H/E). The stained tissue samples were observed and imaged (two slides from each tissue sample) under high resolution light optical microscopy (Keyence Microscope BZ-X800, Keyence Corporation of America, IL, USA). The obtained images were

**Table 1**
Organic compounds identification and quantification of concentrated ambient $PM_{2.5}$.

| PAH | ng/m$^3$ | Alkanes | ng/m$^3$ |
|---|---|---|---|
| Fluorene | 1.95 | n-Tridecane (nC13) | 307.12 |
| Phenanthrene | 6.70 | n-Tetradecane (nC14) | 1.64 |
| Anthracene | 0.24 | n-Pentadecane (nC15) | 59.40 |
| Fluoranthene | 1.58 | n-Nonadecane (nC19) | 432.83 |
| Pyrene | 1.20 | n-Tricosane (nC23) | 307.44 |
| Benzo[*a*]anthracene | 2.41 | n-Tetracosane (nC24) | 450.58 |
| Benzo[*b*]fluoranthene | 4.97 | n-Pentacosane (nC25) | 11.80 |
| Benzo[*k*]fluoranthene | 9.41 | n-Hexacosane (nC26) | 192.88 |
| Benzo[*j*]fluoranthene | 0.70 | n-Heptacosane (nC27) | 25.99 |
| Benzo[*e*]pyrene | 0.75 | n-Octacosane (nC28) | 195.83 |
| Benzo[*a*]pyrene | 8.52 | n-Nonacosane (nC29) | 284.48 |
| Dibenzo[*a,h*]anthracene | 12.67 | n-Tritricontane (nC33) | 432.65 |
| Benzo[*ghi*]perylene | 13.80 | Phthalates | ng/m$^3$ |
| Coronene | 2.71 | Diisobutyl phthalate | 60.99 |
| Indene[*1,2,3-cd*]pyrene | 13.05 | Di-n-butyl phthalate | 260.29 |
| Chrysene | 2.86 | Di-n-pentyl phthalate | 0.06 |
| Triphenylene | 0.55 | Bis[2-ethyl-hexyl] pthalate | 1516.43 |
| Benzophenone | 9.24 | Dicyclohexyl phthalate | 5.05 |
| Naphthalene | 1.68 | | |
| 9 Fluorenone | 0.18 | | |
| 2-Methyl anthracene | 1.22 | | |
| 1-Methyl anthracene | 0.15 | | |
| Anthraquinone | 1.60 | | |
| Retene | 0.28 | | |

Note: Values represent the average of the 8 weeks of exposure. Values were calculated from at least n = 4 filters.

analyzed to determine the presence of lipids (liver), the number of nucleated cells (muscle and WAT), and the increase of the granularity or the islet size (pancreas) using Image J software (ImageJ, U. S. National Institutes of Health, Bethesda, Maryland, USA).

### 2.8. Statistical analysis

The statistical software Prism 8.0 (GraphPad Software, Inc. US) was used for analysis. All results were expressed as mean ± Standard Error of the Mean (SEM) with n = 6. Data was analyzed by one-way ANOVA followed by Bonferroni post hoc corrections. Western blot data was analyzed using non-parametric Man-Whitney U test. Data was considered significant at $p < 0.05$, $p < 0.001$ or $p < 0.0001$.

## 3. Results

### 3.1. Ambient $PM_{2.5}$ concentration and identification and quantification of chemical components and endotoxin

Concentrations of $PM_{2.5}$ in ambient air and concentrated $PM_{2.5}$ atmospheres were measured over the 8-week exposure period; particle concentration were 33.75 ± 12.40 μg/m$^3$ and 337.5 ± 101.03 μg/m$^3$, respectively. Table 1 shows the average concentration of different organic compounds (polycyclic aromatic hydrocarbons-PAH, alkanes, and phthalates) present in the $PM_{2.5}$ collected from an exposure chamber during routine exposure periods. The most abundant PAHs identified were benzo[*ghi*]perylene, indeno[*1,2,3-cd*]pyrene and dibenzo[*a,h*] anthracene. Alkane species found in high concentrations include tetracosane, nonadecane and tritricontane; the phthalates bis[*2ethylhexyl*] phthalate, di-n-butyl phthalate and diisobutyl phthalate were determined in high concentrations. Table 2 summarizes the elemental and endotoxin concentrations determined in $PM_{2.5}$ over the 8-week exposure period. The most abundant metallic elements were Zn, Al and Mn, whilst the more abundant transition metals were Fe, V and Cu. Endotoxin levels in the concentrated $PM_{2.5}$ was found to be an average of 22.21 EU/m$^3$, a level unlikely to negatively affect the respiratory tract in the general population (Farokhi, et al., 2018) The determined organic and inorganic components in $PM_{2.5}$ in this study are capable of inducing ROS generation and activation of the inflammatory response, local tissue injury and systemic toxic effects, as we have previously reported (Aztatzi-Aguilar et al., 2018).

### 3.2. $PM_{2.5}$ + FRD co-exposure induces leptin release and increase in systemic insulin

Morphometric measurements (abdominal curvature, body weight and length) were used to determine the weight gain, body mass index and the Lee index. The average water consumption was estimated (Table 2 Supplementary information) during the exposure period to determine alterations associated with metabolic disruption induced by FRD and/or $PM_{2.5}$ exposure. No statistically significant changes in the morphometric endpoints measured associated with the exposures was observed; however, an 8% increase in body weight in the $PM_{2.5}$ and $PM_{2.5}$ + FRD group were observed. A significant increase in the water consumption was observed in the FRD and the $PM_{2.5}$ + FRD groups compared with the FA and the $PM_{2.5}$ groups. Inflammatory cytokine release and biochemical metabolic markers were analyzed following the subchronic exposure to FA, $PM_{2.5}$, FRD, or $PM_{2.5}$ + FRD. A full analysis of serum markers IL-1β, TNF- α, leptin, MCP-1, and PAI-1, was performed. We observed a statistically significant increase in leptin levels (Fig. 2A) in the $PM_{2.5}$ + FRD group compared with FA, $PM_{2.5}$, and FRD, at multiple time points throughout the exposure (the FA group during week 1 and 4, the $PM_{2.5}$ group during week 4, and the FRD group during week 1). Other cytokines determined showed no statistically significant differences ().

The levels of fasting glucose, fasting insulin and glucose tolerance (GT) were measured to establish systemic biochemical metabolic changes; a summary of these data is presented in Fig. 2. No significant differences between exposure groups were observed in the levels of fasting glucose, fasting insulin and GT prior to $PM_{2.5}$, FRD and $PM_{2.5}$ + FRD exposure (Fig. 2). On the other hand, statistically significant differences in the fasting glucose levels in weeks 2 and 4 of exposure were observed in the $PM_{2.5}$, the FRD, and the $PM_{2.5}$ + FRD exposed groups compared with the FA group (Fig. 2 B). The $PM_{2.5}$ + FRD group exhibited statistically significant differences at week 4 compared to the $PM_{2.5}$ group (Fig. 2B; marginal increases in the FRD group were also observed during week 4 of the exposure, $p = 0.0766$). Moreover, increased fasting insulin levels were observed during weeks 3, 4, 6 and 8 in the co-exposure $PM_{2.5}$ + FRD group compared with the FA group; during weeks 3 and 4 compared with the $PM_{2.5}$ group; also, a marginal increase difference ($p = 0.0632$) was observed during week 8 between the $PM_{2.5}$ + FRD and the fructose group (Fig. 2C). $PM_{2.5}$ + FRD group showed an increasing trend during the 8-week exposure period in insulin systemic levels. In addition, at the end of the 8-week exposure the GT was determined in all the groups, but no significant differences were observed (Fig. 2 E). All together these results suggest that $PM_{2.5}$ + FRD co-exposure induce a metabolic imbalance initiated by an increase of serum leptin and subsequently followed by systemic hyperinsulinemia.

**Table 2**
Elemental and endotoxin content in concentrated ambient $PM_{2.5}$.

| Metals | ng/m$^3$ | Transition metals | ng/m$^3$ |
|---|---|---|---|
| Li | 2.89 | Fe | 57.93 |
| Al | 14.97 | Ni | 7.27 |
| Mn | 10.56 | Co | 0.185 |
| Zn | 325.93 | Cu | 13.09 |
| As | 1.00 | Mo | 1.12 |
| Se | 3.45 | V | 18.61 |
| Sr | 2.48 | Cr | 4.46 |
| Cd | 0.77 | Other elements | ng/m$^3$ |
| Sn | 3.97 | B | 46.45 |
| Sb | 3.33 | Cs | 0.04 |
| Ba | 4.54 | Endotoxin | 22.21 EU/m$^3$ |
| Hg | 0.25 | | |
| Tl | 0.10 | | |
| Pb | 2.59 | | |
| Bi | 0.18 | | |

Note: Values represent the average of the 8 weeks of exposure. Values were calculated from at least n = 4 filters.

### 3.3. $AT_1R$ activation and Insulin/AKT pathway alteration markers in the lung and insulin-sensitive tissues after $PM_{2.5}$ + FRD co-exposure

We have previously reported the impact of cardiopulmonary effects of the RAS activation from the exposure to $PM_{2.5}$ via the induction of the $AT_1R$ (Aztatzi-Aguilar et al., 2015). The activation of RAS is associated with insulin/AKT pathway modification. The expression of $AT_1R$, as a biomarker of RAS activation, and insulin/AKT pathway proteins (IR-β, IRS and AKT) were assessed in the lung and insulin-sensitive tissues in rats exposed to $PM_{2.5}$, FRD or $PM_{2.5}$ + FRD. Protein expression in lung tissue is shown in Fig. 3 A-D. A significant increase in $AT_1R$ expression was observed in all exposure groups compared to the FA group (Fig. 3A). Phosphorylated IRS (ser307) showed a statistically significant decrease in the FRD group compared with the FA group, and in the $PM_{2.5}$ + FRD group compared with FA, $PM_{2.5}$ and FRD groups (Fig. 3C). We also observed a statistically significant increase in AKT phosphorylation (ser473) levels in the FRD and the $PM_{2.5}$ + FRD groups compared with the FA and the $PM_{2.5}$ groups (Fig. 3D). No significant changes were observed in the IR-β expression (Fig. 3B).

Fructose exposure appears to drive protein expression changes in the liver (Fig. 3 E – H). A statistically significative increase of $AT_1R$ levels in the $PM_{2.5}$ + FRD group compared with both FA and $PM_{2.5}$ groups was observed (Fig. 3E). Furthermore, IR-β protein levels were significantly

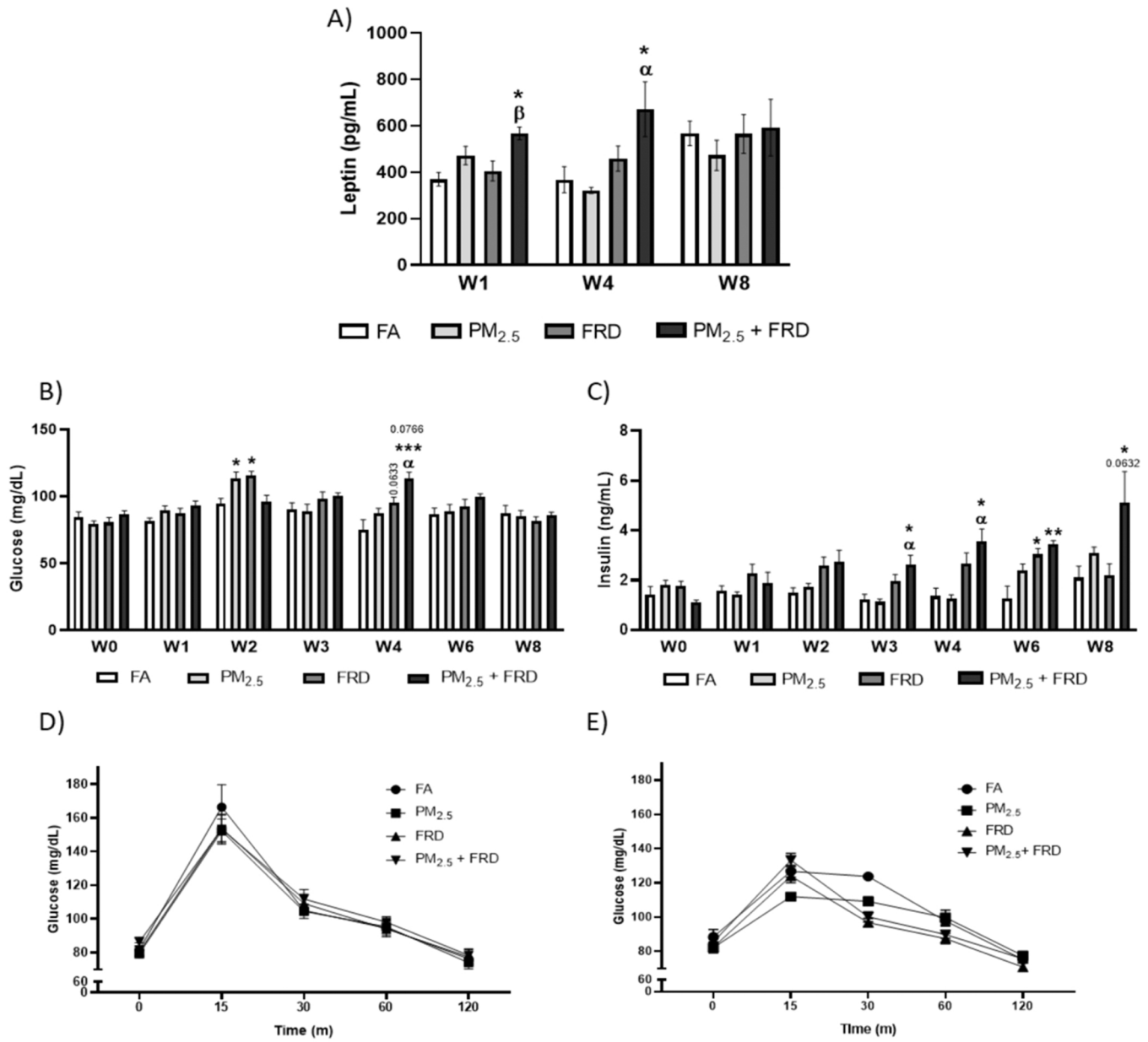


**Fig. 2. Serological determinations during the subchronic exposure.** During some weeks, the blood markers leptin (A), fasting glucose (B) and fasting insulin (C) were determined. Before (D) and at the end (E) of the exposure a glucose tolerance test was performed to all the exposed groups. Data are expressed as mean ± SEM, n = 6. Statistically, significant differences are depicted by $^{*}p = 0.05$ vs. FA, $^{**}p = 0.001$ vs FA, $^{***}p = 0.0001$ vs FA, $^{\alpha}p = 0.05$ vs $PM_{2.5}$, $^{\beta}p = 0.05$ vs FRD by one way ANOVA and post-hoc Bonferroni test.

increased in the FRD group compared with the FA and the $PM_{2.5}$ groups (Fig. 3F), while a statistically significative increase of the AKT phosphorylation was observed in the FRD group compared with the FA group. We also observed a marginal increase in the FRD group compared with the $PM_{2.5}$ group ($p = 0.0703$) and the $PM_{2.5}$ + FRD group compared with the FA group ($p = 0.0701$) (Fig. 3H).

AKT phosphorylation levels were measured in the posterior limb skeletal muscle tissue (Fig. 3 I – L). A significant increase was observed in the fructose-associated groups compared with the FA group (Fig. 3L) but no significant changes were detected in the insulin/AKT pathway or the $AT_1R$ protein levels of the WAT (Fig. 3 M – P). Disruption of the insulin/AKT pathway related proteins in insulin-sensitive tissues can be associated with metabolic imbalance and consequential tissue damage in the affected organs. This disruption could be caused by an established hyperinsulinemic state initiated by $AT_1R$ activation in organs involved in the homeostatic control of the RAS such as the lung and liver.

### 3.4. Histological changes in insulin-sensitive tissues after the exposure to $PM_{2.5}$ + FRD

Histological H/E analysis was performed on insulin-sensitive tissues to determine the possible pathomorphological changes resulting from metabolic imbalance in the insulin/AKT pathway. Tissue samples from liver, skeletal muscle, and WAT were observed under high resolution light optical microscopy. Liver micrographs from the $PM_{2.5}$ (Fig. 4B), FRD (Fig. 4C) and the $PM_{2.5}$ + FRD (Fig. 4D) groups showed the presence of lipids around the hepatocytes (blanks marked by red circles) compared with the FA group (Fig. 4A), where the blanks are not observed. Analysis of the skeletal muscle micrographs showed increased polymorphonucleated cells (recruited inflammatory cells) in all exposure groups (Fig. 4F – H; black circles) with myofibrils distortion (black arrows) exhibited in FRD and $PM_{2.5}$ + FRD groups (Fig. 4G, H). The morphology and the increase in nucleated cells of the skeletal muscle

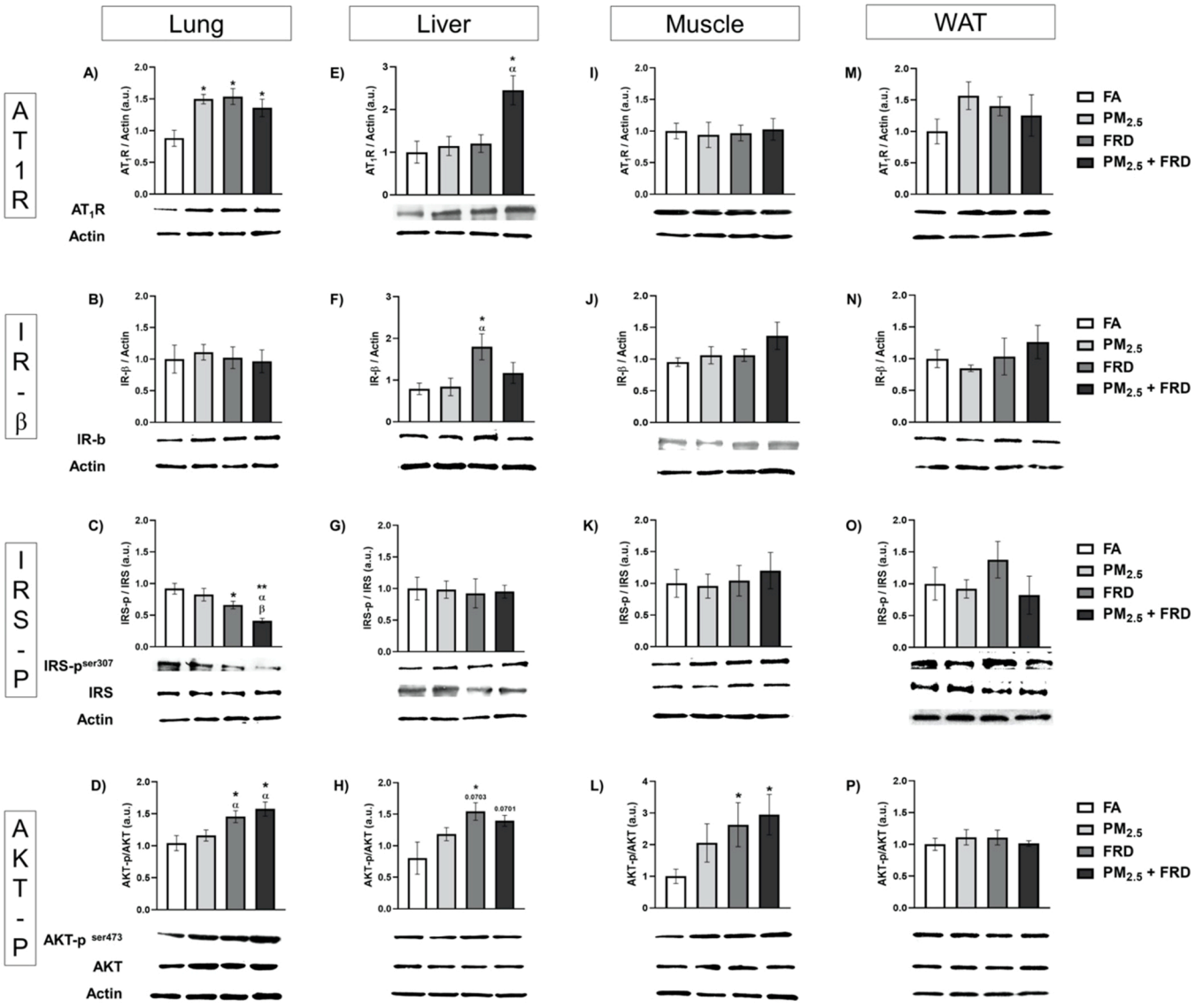


**Fig. 3. Insulin/AKT pathway and $AT_1R$ protein expression after the sub-chronical exposure.** The expression from the insulin/AKT pathway proteins IRS, IR-β and AKT; and the AT1R were determined in lung (A-D), liver (E-H), skeletal muscle (I-L) and white adipose tissue (M-P). Data are expressed as mean ± SEM, n = 6. Statistically, significant differences are depicted by $*p = 0.05$ vs. FA, $**p = 0.001$ vs FA, $^{\alpha}p = 0.05$ vs $PM_{2.5}$, $^{\beta}p = 0.05$ vs FRD; by U-Mann Whitney comparison test.

tissue in the $PM_{2.5}$ + FRD group was more evident than in the other exposure groups. The FA group (Fig. 4E) showed the typical structure of the skeletal muscle. The presence of infiltrated cells between the adipocytes (brown circles) in the $PM_{2.5}$ (Fig. 4J), FRD (Fig. 4K) and the $PM_{2.5}$ + FRD (Fig. 4L) groups were observed in the WAT micrographs. The observed changes in the insulin-sensitive tissues can be related to systemic hyperinsulinemia and insulin/AKT pathway disruption. Also, changes in tissue structure are associated with $PM_{2.5}$ or FRD exposure while changes in liver structure (steatosis) can be a consequence of the FRD and subsequent fructose metabolism. Additionally, skeletal muscle alterations (i.e., myofibrils distortion) can be generated by increases in AKT-p leading to excess metabolism in the muscle. Lastly, increases in cell numbers within the tissues can result from the leptin increase induced by $PM_{2.5}$ or FRD exposure. These results highlight that $PM_{2.5}$ + FRD exposure induces more prominent tissue injury.

### 3.5. $PM_{2.5}$ + FRD induces insulin resistance (IR) and initiates cell damage in pancreatic tissue

Homeostasis Model Assessment of IR (HOMA-IR) and HOMA-β indexes are used to estimate insulin sensitivity and β-cell function from fasting plasma glucose and insulin concentrations (Wallace et al., 2004). The HOMA indexes were determined during the 8-week exposure period to assess the possible imbalance between the insulin circulatory concentrations and the β-cell function. Histopathologic analysis of the pancreatic islets was performed to evaluate the general state of the pancreas insulin production unit. Statistically signigicant increasesse were identified in HOMA-IR during weeks 3, 4, 6 and 8 in the $PM_{2.5}$ + FRD group compared with the FA or the $PM_{2.5}$ groups (Fig. 5A). Marginal differences were observed during weeks 4 and 8 between the FRD and $PM_{2.5}$ + FRD groups ($p = 0.087$ and $p = 0.0732$, respectively). No significant differences were detected in HOMA-β levels (Fig. 5B).

The pancreas in all exposure groups exhibited normal external (acinar cells) and internal (Islets of Langerhans) structure. Chromatin fragments (small nuclear granules) were observed in the nucleus of pancreatic islets cells of the $PM_{2.5}$ (Fig. 5D), FRD (Fig. 5E), and the $PM_{2.5}$ + FRD (Fig. 5F) groups with less chromatin fragments seen in the FA group (Fig. 5C). The micrographs (20x) showed a difference in the Langerhans islets size (Fig. 2 Supplementary) indicating an increasing trend in the size of islets in the $PM_{2.5}$ and FRD groups. Our results

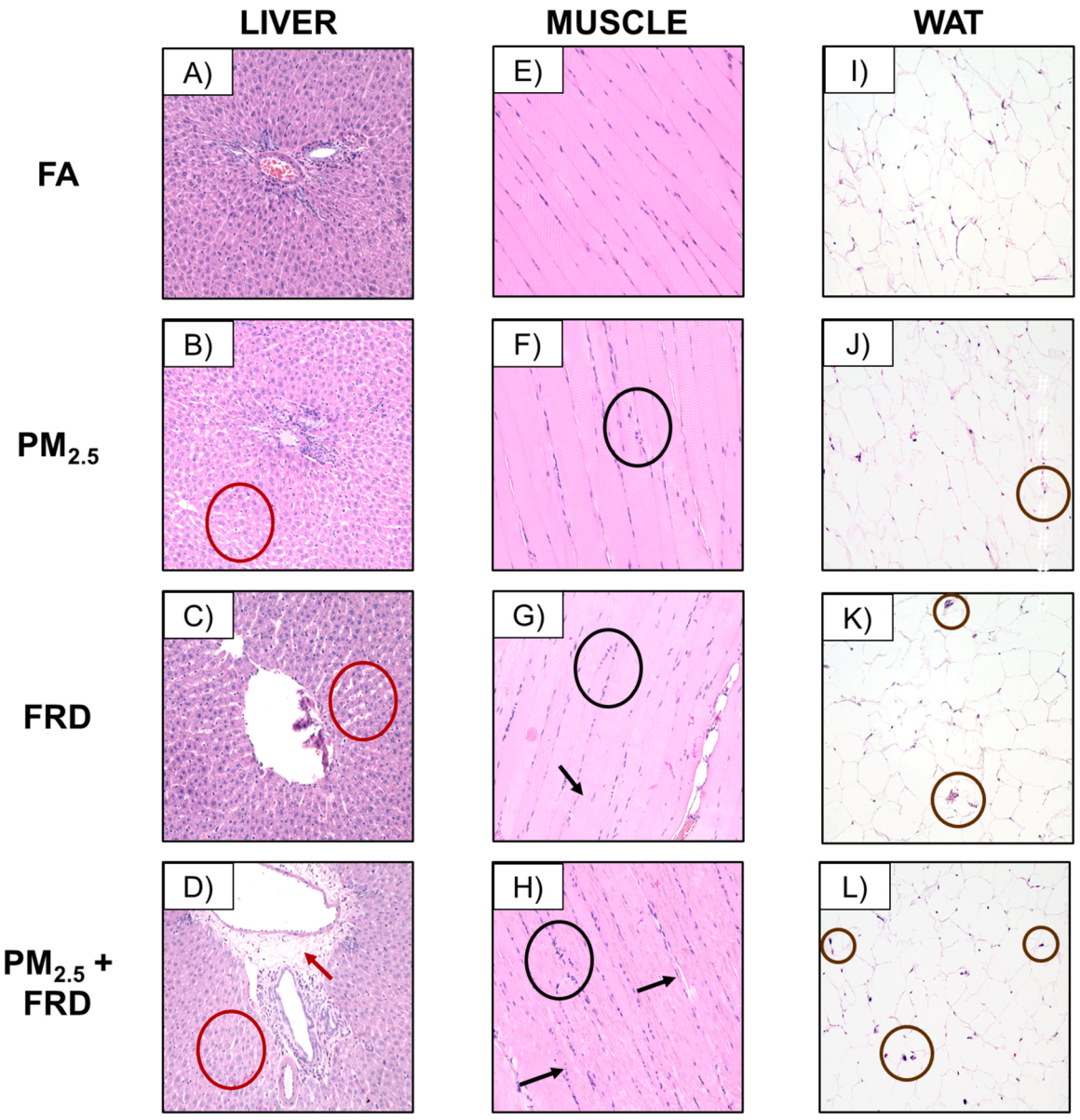


**Fig. 4. Insulin-sensitive tissues structural changes after the $PM_{2.5}$ and/or FRD sub-chronical exposure.** Histological images (20x) from the insulin sensitive tissues liver (A-D), skeletal muscle (E-H) and white adipose tissue (I-L) were obtained after the $PM_{2.5}$ and/or FRD sub-chronical exposure. Changes in the tissues are depicted by circles and arrows. Red circles showed the generated lipidosis in liver; black circles showed the increased cellularity meanwhile black arrows mark the tissue changes in skeletal muscle; and brown circles showed the cellular infiltration between the adipocytes.

suggest that $PM_{2.5}$ + FRD co-exposure results in systemic insulin resistance leading to increased HOMA-IR index.

## 4. Discussion

Exposure to environmental pollutants such as $PM_{2.5}$ together with lifestyle and diet can contribute to the progression of metabolic disruption and insulin resistance, however, the mechanisms involved are not completely comprehended. We investigated metabolic and inflammation-related responses in rats exposed to FRD, $PM_{2.5}$ and a $PM_{2.5}$ + FRD co-exposure. Increases in leptin levels, hyperinsulinemia, increase of the $AT_1R$ receptor protein level, the disruption of the insulin/AKT pathway and pathomorphological injury in the liver, skeletal muscle and WAT leading to an insulin resistance state were observed in male Sprague Dawley rats after a subchronic exposure to $PM_{2.5}$ + FRD. These changes are consistent with the induction of metabolic syndrome and insulin resistance.

$PM_{2.5}$ constituents measured in this study can be contributing factors in the development of insulin resistance and metabolic imbalance. Organic components in ambient $PM_{2.5}$, such as PAHs, have been correlated with increased fasting glucose levels, metabolic syndrome and different dyslipidemias in adolescents and the general population (Ma et al., 2019; Li et al., 2021). Urinary concentrations of different phthalates and metabolites have also been positively associated with glycosylated hemoglobin, increased fasting glucose, insulin, HOMA-IR and HOMA-β in humans (Dales et al., 2018). In addition, the elemental fraction of heavy metals, such as As can induce insulin/AKT pathway disruption pancreas, while Cd increases fasting glucose levels in Sprague Dawley rats (Chen et al., 2009). On the other hand, Ni exacerbates the effects of IR in male apolipoprotein A (Apo-E) knockout mice exposed to $PM_{2.5}$ by elevating fasting glucose levels and HOMA-IR index (Xu et al., 2012). Furthermore, endotoxin can generate tissue specific inflammation and lead to hyperinsulinemia and increased levels of fasting glucose which generate an insulin resistance condition (Cani et al., 2007).

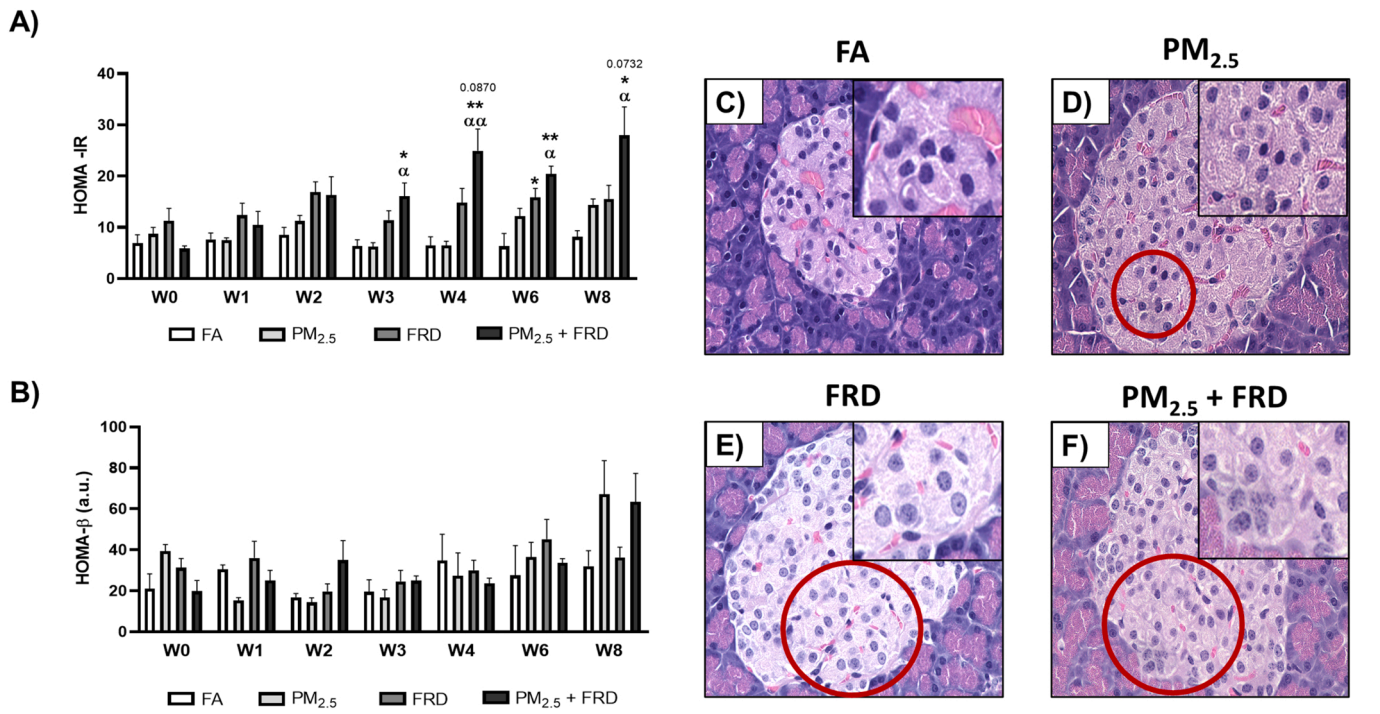


**Fig. 5. HOMA indexes values and pancreatic tissue histology during the sub-chronical exposure.** Based on the fasting glucose and insulin values obtained the HOMA-β (A) and the HOMA-IR (B) were calculated in several weeks. Also, histological images (60x) from the pancreas were obtained from FA (C), $PM_{2.5}$ (D), FRD (E) and $PM_{2.5}$ + FRD (F) exposed groups. Circles in the images showed the presence of apoptotic cells in the pancreatic islets. Data are expressed as mean ± SEM, n = 6. Statistically, significant differences are depicted by $*p = 0.05$ vs. FA, $**p = 0.001$ vs FA, $^{\alpha}p = 0.05$ vs $PM_{2.5}$, $^{\alpha\alpha}p = 0.001$ vs $PM_{2.5}$ by one way ANOVA and post-hoc Bonferroni test.

Inflammatory responses have been associated with metabolic changes in other studies. The increase of inflammatory markers like leptin, IL-6, IL-1β or TNF-α have been directly related to IR and diabetes development (Jager et al., 2007). Moreover, inflammatory factors elicited by exposure to ambient $PM_{2.5}$ contribute to diabetogenic effects functioning as enhancers of insulin resistance in insulin-sensitive tissues (Long et al., 2020). Leptin, participates in glucose homeostasis, hepatic insulin sensitivity, and glucose uptake by peripheral tissues (Amitani et al., 2013) and acts as a mediator of inflammation from multifactorial origins and is released by adipocytes (Chen et al., 2015). Machado Campolim et al. (2020) exposed mice to $PM_{2.5}$ (600 μg/$m^3$ per day) for 12 weeks, and showed an increase in serum leptin, fasting insulin and HOMA-IR index. We observed a statistically significant increase in systemic leptin release in the $PM_{2.5}$ + FRD group, and no significant changes in the acute inflammatory phase cytokines (Fig. 1 Supplementary). This observation suggests the development of a low-grade inflammation in weeks 1 and 4, which has been related with metabolic diseases, and could have resolved by the end of the 8-week exposure period.

Exposure to ambient $PM_{2.5}$ has been shown to illicit systemic alterations in metabolic processes. In this study, we observed a statistically significant increase of fasting glucose at week 2 in the $PM_{2.5}$ and FRD groups, and at week 4 in $PM_{2.5}$ + FRD (Fig. 2B). In a similar study performed on C57BL/6 male mice, no metabolic alterations were observed following 8-week (subchronic) exposure to $PM_{2.5}$ and a high fat diet (Liu et al., 2014). However, in this same study found that chronic exposure (17-week) induced a whole-body IR, which it is characterized by increases in fasting glucose levels and HOMA-IR index, decreased HOMA-β function, abnormal glucose tolerance, and attenuation of whole-body insulin sensitivity (Liu et al., 2014). Additionally, a chronic $PM_{2.5}$ exposure (3 month) of Apo-E deficient male mice reported the induction of IR indicated by higher glucose levels and HOMA-IR values (Xu et al., 2012). In the same manner, we did not observe changes in the GT after 8 weeks of exposure to $PM_{2.5}$, FRD or $PM_{2.5}$ + FRD indicating that glucose metabolism was not affected. These findings suggest that changes in systemic glucose handling could be related with the time of exposure to $PM_{2.5}$ or FRD or $PM_{2.5}$ + FRD.

An increase in fasting insulin in the $PM_{2.5}$ + FRD group from week 3 to week 8, was also observed suggesting systemic hyperinsulinemia. Our observations concur with those reported by Machado Campolim et al. (2020) who observed hyperinsulinemia and IR from chronic $PM_{2.5}$ exposure. Increase in insulin levels can be associated with diverse metabolic transformations and to the initiation of an IR state. In humans, blood insulin levels increase during IR in order to maintain glucose tolerance and is accompanied by activation of metabolic signaling pathways, like the Insulin/AKT pathway in insulin-sensitive tissues (Brierley and Semple, 2021; Ormazabal et al., 2018).

We have previously reported an increase of $AT_1R$ expression in the lung from the exposure to ambient $PM_{2.5}$ that accompanied pulmonary, cardiac and renal damage via the activation of RAS in adult rats (Aztatzi-Aguilar et al., 2015; Aztatzi-Aguilar et al., 2016; Aztatzi-Aguilar et al., 2018). In our study we observe an increase in the $AT_1R$ in the lung was observed following the exposure to $PM_{2.5}$, FRD and $PM_{2.5}$ + FRD, and in the liver after $PM_{2.5}$ + FRD exposure. Upregulating of $AT_1R$ receptor and its down-stream signaling pathway have been associated with insulin resistance progression (in insulin sensitive tissues), where the activation of Rho kinases inhibits the insulin/AKT pathway members IRS-1 or AKT (Luther and Brown, 2011; Kim et al., 2012; Forrester et al., 2018). Moreover, the activation of the RAS may induce inflammation, leading to liver disfunction manifested by steatosis, lipid metabolism dysregulation and the development of insulin resistance (Hussain et al., 2017; Pizoń et al., 2018). The induction of $AT_1R$ in the lung and the liver, specifically as a response to the $PM_{2.5}$ + FRD suggests a contribution to the activation of the RAS in systemic insulin levels. To evaluate the perturbation on the insulin/AKT pathway the expression of IR-β, IRS and AKT were assessed in the lung (initial contact organ of $PM_{2.5}$ exposure) and insulin sensitive tissues (liver, skeletal muscle, white adipose) that play an essential role in glucose transport and metabolism.

In the lung, the increase of AKT-p and the decrease of IRS-p were observed in FRD and $PM_{2.5}$ + FRD groups. AKT protein activation and its down-stream pathway can be associated to the survival and proliferative cellular functions in the lung as a consequence of tissue injury (Xu et al., 2012). Furthermore, a study of $PM_{2.5}$ exposure (300 μg total intratracheal exposure) in ICR mice showed an increase in inflammatory response in lungs (cellular infiltration and IL-1 increase) mediated by Rac1/AKT signaling pathway (Zhang et al., 2019). Our results show that exposure to $PM_{2.5}$ in combination with FRD increased this imbalance in the insulin/AKT signaling pathway, which could be associated with the local injury and inflammatory response to $PM_{2.5}$ in lungs.

In insulin-sensitive tissues where the modification of AKT pathway is related to metabolic diseases, different changes were observed in the FRD and $PM_{2.5}$ + FRD groups denoted by the increase in AKT phosphorylation in liver and skeletal muscle, but not in WAT. The activation of the insulin/AKT pathway in the liver inhibits gluconeogenesis and induce glucose uptake and general protein synthesis; (Manning and Toker, 2017). In skeletal muscle an overload of glucose uptake can promote a sustained fibrillar contraction leading to the increase of protein synthesis and fibrillar damage (Egerman and Glass, 2014). In addition, circulatory glucose can participate in insulin processes mainly in skeletal muscle rather than in adipose tissue via AKT activation (Jaiswal et al., 2019).

Different histopathological alterations in tissues can be related with tissue-specific inflammatory responses. A 24-week exposure to $PM_{2.5}$ ($115 \pm 1.5$ μg/m$^3$ or $230 \pm 2.5$ μg/m$^3$) showed an increase of lipid synthesis and accumulation in the liver; which was associated to oxidative and inflammatory processes (Xu et al., 2019). The pathomorphological damage observed in liver, skeletal muscle, WAT, and pancreas showed the effect of $PM_{2.5}$ or FRD exposure (Fig. 4). Liver steatosis can be related to the tissue inflammatory response and $AT_1R$ activation while inflammatory responses in liver may related to $PM_{2.5}$ or FRD exposure. We observed $AT_1R$ activation was only observed in the $PM_{2.5}$ + FRD group where a concomitant increase in lipids was also observed, compared to the FA group. Moreover, a sustained increase of pro-inflammatory cytokines may inhibit the normal myogenic progression leading to tissue damage in skeletal muscle (Howard et al., 2020); the presence of cellular infiltration and fibrillar damage in skeletal muscle can be associated with the onset of an inflammatory response in the tissue. As previously mentioned, AKT-p induced by FRD exposure in skeletal muscle may contribute to fibrillar damage leading to the intensified effect seen in the $PM_{2.5}$ + FRD group. Increased levels of leptin have been associated with increases in TNF-α and IL-1β and the recruitment of immune cells (Jung and Choi, 2014). Leptin is synthetized in adipose tissue and can recruit different inflammatory cells to this tissue, so the increase of leptin in the $PM_{2.5}$ + FRD can be directly associated with the presence of cellular infiltration. Together, the inflammation and structural damages of the insulin-sensitive tissues, accompanied with the induction of AKT-p, activation of $AT_1R$ and systemic hyperinsulinemia, can contribute to a state of insulin resistance.

Different cell death mechanisms can be involved in pancreatic β cells damage during insulin resistance. Activation of cell death can occur, in part, due to increases in the inflammatory response and subsequent activation down-stream pathways activation, glucotoxicity, and lipotoxicity leading to pyroptosis or apoptosis which can induce DNA fragmentation (Cnop et al., 2005; Rojas et al., 2018). DNA fragmentation in β-pancreatic cells, which account for 70% of the cells in the Islets of Langerhans, was evident in all the exposure groups. However, our semi-quantitative analysis showed increased fragmentation in the $PM_{2.5}$ and $PM_{2.5}$ + FRD groups indicating that $PM_{2.5}$ exposure may stimulate cellular damage to a greater extent than FRD diet alone.

The HOMA-IR has proven to be a robust tool for the surrogate assessment of IR (Gayoso-Diz et al., 2013). Meanwhile, HOMA-β is related with β-cell response or pancreatic insulin secretion (Vasudha et al., 2016). The values from the HOMA-IR index in the co-exposure group showed an increase compared with the other groups demonstrating insulin resistance. However, no changes in the HOMA-β were observed in all the groups, demonstrating no loss of the β cells function and a sustained secretion of insulin. It is important to consider the histological observations in the pancreas (associated to cell death) and the increase in the fasting insulin measured in the $PM_{2.5}$ + FRD group as these changes may be associated with alterations in subsequent insulin production and the possible tissue damage. Based on these results, $PM_{2.5}$ + FRD co-exposure increases the synthesis of insulin measured in pancreatic β cells, initiates modification of the insulin/AKT signaling pathway, and damages the insulin sensitive tissues and the systemic insulin resistance state in Sprague Dawley rats.

## 5. Limitations of the study

It is important to consider some limitations of our study. Particulate matter chemical speciation has been statistically correlated with specific biological effects (cytokines and proteins modification) generated in vitro (Zheng et al., 2019). In our work the chemical speciation and concentration of the particulate matter was determined, and a descriptive analysis of the metabolic effects caused by some of the obtained compounds was performed. Nevertheless, the statistical correlation between the compounds present in the particulate matter and the different modified biological markers could give more information about the participation of specific compounds involved in metabolic damage. The inflammatory response generated during IR and metabolic diseases (diabetes, obesity, metabolic syndrome) is considered as 'low-grade inflammation' and increases in these markers can be tissue specific (Jung and Choi, 2014). Determination of inflammatory markers like TNF-α, IL-1β, IL-6, among others in the insulin sensitive tissues could contribute to the understanding of the modification of inflammatory pathways and their relationship with the IR in these tissues. Chronic $PM_{2.5}$ exposure can generate sex-dependent IR and lipidic metabolism modifications; female rodents have been found to be more susceptible to lipid accumulation and IR than males (Li et al., 2020). Our study was based in previous investigations performed in our laboratory centered on the systemic effects of $PM_{2.5}$ in male rats. However, future studies should aim to also determine the biological, pathophysiological, and metabolic effect caused by $PM_{2.5}$ and the FRD in female rats.

## 6. Conclusions

Our results show a systemic IR induced from $PM_{2.5}$ + FRD co-exposure. The main pathophysiological manifestations are hyperinsulinemia, the insulin/AKT disruption and tissue damage in the pancreas and in insulin-sensitive tissues. These findings indicate a collaborative effect of the FRD with $PM_{2.5}$, a ubiquitous environmental pollutant, thereby establishing that concomitant exposure to these metabolic disease risk factors can significantly impair health and contribute to the diabetic pandemic in highly polluted locations.

Other factors that induce insulin resistance should be evaluated further. Different downstream proteins from the insulin/AKT pathway (FOXO proteins, GLUT transporters, among others); and the possible participation of other pathways like JAK-STAT and MAK kinases can be investigated to better understand the insulin resistance state in the glucose transport, lipids, and glycogen synthesis. Therefore, it is important to evaluate the organ-systems crosstalk, where other organs (brain, heart, spleen, kidney, reproductive organs) could be affected by the increase of circulatory insulin (Oishi and Manabe, 2020; Ormazabal et al., 2018). We observed that $PM_{2.5}$ + FRD co-exposure increases the fragmentation of DNA in pancreatic β cells. Studying the pathways involved in cell death (caspase liberation, p53, Bax or Bcl-2 families) can help further the knowledge surrounding this type of cell damage and explicate relationships with the insulin levels observed.

## Ethics approval

The Internal Committee for the Use and Care of Laboratory Animals, Cinvestav, approved all animal procedures in accordance with the "Principles of Laboratory Animal Care" guidelines under protocol No. 0312–20.

## Funding

This work was supported by Consejo Nacional de Ciencia y Tecnología (Conacyt)-México, Grant No. 286739, Convocatoria Ciencia Básica 2016 and partially supported by NHLBI, Grant No. 3RO1HL-144258-02S1. AJC held a Conacyt Ph.D. Fellowship No. 780827.

## CRediT authorship contribution statement

**Arturo Jiménez-Chávez:** Conceptualization, Visualization, Methodology, Formal analysis, Investigation, Writing – original draft. **Russell Morales-Rubio:** Methodology, Investigation, Validation, Formal analysis. **Eliu Sánchez-Gasca:** Methodology, Investigation. **Mónica Rivera-Rosas:** Methodology, Investigation. **Marisela Uribe-Ramírez:** Methodology, Investigation, Validation. **Omar. Amador-Muñoz:** Methodology, Investigation, Validation.**Y. Margarita Martínez-Domínguez:** Methodology, Investigation. **Irma Rosas-Perez:** Methodology, Investigation, Validation. **Elizabeth H. Choy:** Methodology, Investigation. **David A. Herman:** Conceptualization, Writing – original draft, Supervision. **Michael T. Kleinman:** Conceptualization, Writing – original draft, Resources, Supervision, Fundings acquisition. **Andrea De Vizcaya-Ruiz:** Conceptualization, Visualization, Writing – original draft, Resources, Supervision, Project administration, Fundings acquisition.

## Declaration of Competing Interest

The authors declare that they have no known competing financial interests or personal relationships that could have appeared to influence the work reported in this paper.

## Data Availability

Data will be made available on request.

## Acknowledgement

We acknowledge the excellent technical assistance of Ángel Barrera Hernández and the LISTO (Research and Toxicology Analysis Laboratory), Cinvestav-Zacatenco, Mexico for the elemental analysis composition of $PM_{2.5}$. We also acknowledge the assistance of Victor Hugo Olivera Rodríguez from Laboratorio de Patologia Molecular e Inmunohistoquimica, Instituto Nacional de Cancerologia, México for histopathological sample preparation.

## Appendix A. Supporting information

Supplementary data associated with this article can be found in the online version at doi:10.1016/j.etap.2023.104115.

## References

Amitani, M., Asakawa, A., Amitani, H., Inui, A., 2013. The role of leptin in the control of insulin-glucose axis. Front. Neurosci. 7 (7), 1–12. https://doi.org/10.3389/fnins.2013.00051.

Aztatzi-Aguilar, O.G., Uribe-Ramírez, M., Narváez-Morales, J., De Vizcaya-Ruiz, A., Barbier, O., 2016. Early kidney damage induced by subchronic exposure to PM2.5 in rats. Part. Fibre Toxicol. 13 (1), 68.

Aztatzi-Aguilar, O.G., Valdés, A., Valdés-Arzate, V., Debray-García, Y., Calderó N-Aranda, E.S., Uribe-Ramirez, M., De Vizcaya-Ruiz, A., 2018. Exposure to ambient particulate matter induces oxidative stress in lung and aorta in a size-and time-dependent manner in rats. Toxicol. Res. Appl. Toxicol. Res. Appl. 2, 1–15. https://doi.org/10.1177/2397847318794859.

Aztatzi-Aguilar, Octavio Gamaliel, Uribe-Ramírez, M., Arias-Montaño, J.A., Barbier, O., De Vizcaya-Ruiz, A., 2015. Acute and subchronic exposure to air particulate matter induces expression of angiotensin and bradykinin-related genes in the lungs and heart: angiotensin-II type-I receptor as a molecular target of particulate matter exposure. Part. Fibre Toxicol. 12 (1), 1–18.

Beristain-Montiel, E., Villalobos-Pietrini, R., Arias-Loaiza, G.E., Gómez-Arroyo, S.L., Amador-Muñoz, O., 2016. An innovative ultrasound assisted extraction micro-scale cell combined with gas chromatography/mass spectrometry in negative chemical ionization to determine persistent organic pollutants in air particulate matter. J. Chromatogr. A 1477, 100–107. https://doi.org/10.1016/j.chroma.2016.11.043.

Boucher, J., Kleinridders, A., Kahn, C.R., 2014. Insulin Receptor Signaling in Normal and insulin-resistant state. Cold Spring Harb. Perspect. Biol. 2014 (6), a009191. https://doi.org/10.1101/cshperspect.a009191.

Bray, G., Nielsen, S., Popkin, B., 2004. Consumption of high-fructose corn syrup in beverages may play a role in the epidemic of obesity. Am. J. Clin. Nut. 79, 537–543. https://doi.org/10.1093/ajcn/79.4.537.

Brierley, G.V., & Semple, R.K. (2021). Insulin at 100 years – is rebalancing its action key to fighting obesity-related disease ?, 1–7. https://doi.org/10.1242/dmm.049340.

Burnette, W., 1981. "Western Blotting": Electrophoretic transfer of proteins from sodium dodecyl sulfate-polyacrylamide gels to unmodified nitrocellulose and radiographic detection with antibody and radioiodinated protein A. Anal. Biochem. 112, 195–203. https://doi.org/10.1016/0003-2697(81)90281-5.

Cani, P.D., Amar, J., Iglesias, M.A., Poggi, M., Knauf, C., Bastelica, D., Alessi, M.C., 2007. Metabolic endotoxemia initiates obesity and insulin resistance. Diabetes 56 (July), 1761–1772. https://doi.org/10.2337/db06-1491.P.D.C.

Cervantes-Martínez, K., Stern, D., Zamora-Muñoz, J.S., López-Ridaura, R., Texcalac-Sangrador, J.L., Cortés-Valencia, A., Riojas-Rodríguez, H., 2022. Air pollution exposure and incidence of type 2 diabetes in women: a prospective analysis from the Mexican Teachers' Cohort. Sci. Total Environ. 818, 151833 https://doi.org/10.1016/J.SCITOTENV.2021.151833.

Chen, L., Chen, R., Wang, H., Liang, F., 2015. Mechanisms linking inflammation to insulin resistance. Int. J. Endocrinol. *2015*. https://doi.org/10.1155/2015/508409.

Chen, Y.W., Yang, C.Y., Huang, C.F., Hung, D.Z., Leung, Y.M., Liu, S.H., 2009. Heavy metals, islet function and diabetes development. Islets 1 (3), 169–176. https://doi.org/10.4161/isl.1.3.9262.

Chilian-Herrera, O.L., Tamayo-Ortiz, M., Texcalac-Sangrador, J.L., Rothenberg, S.J., López-Ridaura, R., Romero-Martínez, M., Téllez-Rojo, M.M., 2021. PM2.5 exposure as a risk factor for type 2 diabetes mellitus in the Mexico City metropolitan area. BMC Public Health 21 (1), 1–10. https://doi.org/10.1186/s12889-021-12112-w.

Cnop, M., Welsh, N., Jonas, J., Jo, A., Lenzen, S., 2005. Mechanisms of pancreatic b-cell death in type 1 and type 2 diabetes Many Differences. Few Similar *Am. Diabetes Assoc.* 6, 97–107. https://doi.org/10.2337/diabetes.54.suppl_2.s97.

Collares-Buzato, C.B., 2016. High-fat diets and β-cell dysfunction: molecular aspects. Mol. Nutr. Diabetes A Vol. Mol. Nutr. Ser. 115–130. https://doi.org/10.1016/B978-0-12-801585-8.00010-5.

Dales, R.E., Kauri, L.M., Cakmak, S., 2018. The associations between phthalate exposure and insulin resistance, β-cell function and blood glucose control in a population-based sample. Sci. Total Environ. 612, 1287–1292. https://doi.org/10.1016/j.scitotenv.2017.09.009.

Egerman, M.A., Glass, D.J., 2014. Signaling pathways controlling skeletal muscle mass. Crit. Rev. Biochem. Mol. Biol. 49 (1), 59–68. https://doi.org/10.3109/10409238.2013.857291.

Falcon-Rodriguez, C.I., De Vizcaya-Ruiz, A., Rosas-Pérez, I.A., Osornio-Vargas, Á.R., Segura-Medina, P., 2017. Inhalation of concentrated PM2.5 from Mexico City acts as an adjuvant in a guinea pig model of allergic asthma. Environ. Pollut. 228, 474–483. https://doi.org/10.1016/j.envpol.2017.05.050.

Forrester, S.J., Booz, G.W., Sigmund, C.D., Coffman, T.M., Kawai, T., Rizzo, V., Eguchi, S., 2018. Angiotensin II signal transduction: an update on mechanisms of physiology and pathophysiology. Physiol. Rev. 98 (3), 1627–1738. https://doi.org/10.1152/physrev.00038.2017.

Freeman, A.M., Pennings, N., 2022. Insulin Resistance. [Updated 2022 Jul 4]. StatPearls. Treasure Island (FL): StatPearls Publishing. Jan-. Available from: https://www.ncbi.nlm.nih.gov/books/NBK507839/.

Gayoso-Diz, P., Otero-González, A., Rodriguez-Alvarez, M.X., Gude, F., García, F., De Francisco, A., Quintela, A.G., 2013. Insulin resistance (HOMA-IR) cut-off values and the metabolic syndrome in a general adult population: effect of gender and age: EPIRCE cross-sectional study. BMC Endocr. Disord. 13 (Cvd) https://doi.org/10.1186/1472-6823-13-47.

Haberzettl, P., O'Toole, T.E., Bhatnagar, A., Conklin, D.J., 2016. Exposure to fine particulate air pollution causes vascular insulin resistance by inducing pulmonary oxidative stress. Environ. Health Perspect. 124 (12), 1830–1839. https://doi.org/10.1289/EHP212.

Herman, D.A., Wingen, L.M., Johnson, R.M., Keebaugh, A.J., Renusch, S.R., Hasen, I., Kleinman, M.T., 2020. Seasonal effects of ambient PM2.5 on the cardiovascular system of hyperlipidemic mice. J. Air Waste Manag. Assoc. https://doi.org/10.1080/10962247.2020.1717674.

Hill, B.G., Rood, B., Ribble, A., & Haberzettl, P. (2021). Fine particulate matter (PM 2.5) inhalation-induced alterations in the plasma lipidome as promoters of vascular inflammation and insulin resistance. https://doi.org/10.1152/ajpheart.00881.2020.

Howard, E.E., Pasiakos, S.M., Blesso, C.N., Fussell, M.A., Rodriguez, N.R., 2020. Divergent roles of inflammation in skeletal muscle recovery from injury. Front. Physiol. 11, 1–13. https://doi.org/10.3389/fphys.2020.00087.

Huang, X., Liu, G., Guo, J., Su, Z.Q., 2018. The PI3K/AKT pathway in obesity and type 2 diabetes. Int. J. Biol. Sci. 14 (11), 1483–1496. https://doi.org/10.7150/ijbs.27173.

Hussain, S.A., Utba, R.M., Assumaidaee, A.M., 2017. Effects of azilsartan, aliskiren or their combination on high fat diet-induced non-alcoholic liver disease model in rats. Med. Arch. 71 (4), 251–255. https://doi.org/10.5455/medarh.2017.71.251-255.

Jaiswal, N., Gavin, M.G., Iii, W.J.Q., Luongo, T.S., Gelfer, R.G., Baur, J.A., Titchenell, P. M., 2019. The role of skeletal muscle Akt in the regulation of muscle mass and glucose homeostasis. Mol. Metab. 28, 1–13. https://doi.org/10.1016/j.molmet.2019.08.001.

Jung, U.J., Choi, M.S., 2014. Obesity and its metabolic complications: The role of adipokines and the relationship between obesity, inflammation, insulin resistance, dyslipidemia and nonalcoholic fatty liver disease. Int. J. Mol. Sci. 15 (4), 6184–6223. https://doi.org/10.3390/ijms15046184.

Kim, J.A., Jang, H.J., Martinez-Lemus, L.A., Sowers, J.R., 2012. Activation of mTOR/p70S6 kinase by ANG II inhibits insulin-stimulated endothelial nitric oxide synthase and vasodilation. Am. J. Physiol. - Endocrinol. Metab. 302 (2), 201–208. https://doi.org/10.1152/ajpendo.00497.2011.

Kim, S., Jaques, P.A., Chang, M., Froines, J.R., Sioutas, C., 2001. Versatile aerosol concentration enrichment system (VACES) for simultaneous in vivo and in vitro evaluation of toxic effects of ultrafine, fine and coarse ambient particles Part I: Development and laboratory characterization. J. Aerosol Sci. 32 (11), 1281–1297. https://doi.org/10.1016/S0021-8502(01)00057-X.

Kleinman, M.T., Sioutas, C., Froines, J.R., Fanning, E., Hamade, A., Mendez, L., Oldham, M., 2007. Inhalation of concentrated ambient particulate matter near a heavily trafficked road stimulates antigen-induced airway responses in mice. Inhal. Toxicol. 19 (SUPPL. 1), 117–126. https://doi.org/10.1080/08958370701495345.

Kopp, W., 2019. How western diet and lifestyle drive the pandemic of obesity and civilization. Diseases. https://doi.org/10.2147/DMSO.S216791.

Kruger, N.J., 1996. The bradford method for protein quantitation. Protein Protoc. Handb. 15–20.

Lancaster, K., 2020. Current Intake and Demographic Disparities in the Association of Fructose-Rich Foods and Metabolic Syndrome. Nutrition, Obesity and Exercise 3, 1–3. https://doi.org/10.1001/jamanetworkopen.2020.10224.

Li, K., Yin, R., Wang, Y., Zhao, D., 2021. Associations between exposure to polycyclic aromatic hydrocarbons and metabolic syndrome in U.S. adolescents: cross-sectional results from the National Health and Nutrition Examination Survey (2003–2016) data. Environ. Res. 202, 111747 https://doi.org/10.1016/j.envres.2021.111747.

Li, R., Sun, Q., Lam, S.M., Chen, R., Zhu, J., Gu, W., Liu, C., 2020. Sex-dependent effects of ambient PM2.5 pollution on insulin sensitivity and hepatic lipid metabolism in mice. Part. Fibre Toxicol. 17 (1), 1–14. https://doi.org/10.1186/s12989-020-00343-5.

Liu, C., Xu, X., Bai, Y., Wang, T.Y., Rao, X., Wang, A., Rajagopalan, S., 2014. Air pollution-mediated susceptibility to inflammation and insulin resistance: Influence of CCR2 pathways in mice. Environ. Health Perspect. https://doi.org/10.1289/ehp.1306841.

Long, M. hui, Zhang, C., Xu, D. qun, Fu, W. liang, Gan, X. dong, Li, F., Xu, gang, D., 2020. PM2.5 aggravates diabetes via the systemically activated IL-6-mediated STAT3/SOCS3 pathway in rats' liver. Environ. Pollut. 256 (113342) https://doi.org/10.1016/j.envpol.2019.113342.

Luther, J.M., Brown, N.J., 2011. The renin-angiotensin-aldosterone system and glucose homeostasis. Trends Pharmacol. Sci. 32 (12), 734–739. https://doi.org/10.1016/j.tips.2011.07.006.

Ma, J., Zhou, Y., Liu, Y., Xiao, L., Cen, X., Li, W., Chen, W., 2019. Association between urinary polycyclic aromatic hydrocarbon metabolites and dyslipidemias in the Chinese general population: a cross-sectional study. Environ. Pollut. 245, 89–97. https://doi.org/10.1016/j.envpol.2018.10.134.

Machado Campolim, C., Weissmann, L., Kraüss De Oliveira Ferreira, C., Pizetta Zordão, O., Paula, A., Dornellas, S., Oliveira Prada, P., 2020. Short-term exposure to air pollution (pM 2.5) induces hypothalamic inflammation, and long-term leads to leptin resistance and obesity via Tlr4/Ikbke in mice. *Sci. Rep.* | 10, 10160. https://doi.org/10.1038/s41598-020-67040-3.

MacPhee, D.J., 2010. Methodological considerations for improving Western blot analysis. J. Pharmacol. Toxicol. Methods 61 (2), 171–177. https://doi.org/10.1016/j.vascn.2009.12.001.

Manning, B.D., Toker, A., 2017. AKT/PKB signaling: navigating the network. Cell 169 (3), 381–405. https://doi.org/10.1016/j.cell.2017.04.001.

Matthews, D.R., Hosker, J.P., Rudenski, A.S., Naylor, B.A., Treacher, D.F., Turner, R.C., 1985. Homeostasis model assessment: insulin resistance and beta-cell function from fasting plasma glucose and insulin concentrations in man. Diabetologia 28, 412–419. https://doi.org/10.1007/BF00280883.

Mietelska-Porowska, A., Domańska, J., Want, A., Więckowska-Gacek, A., Chutorański, D., Koperski, M., Wojda, U., 2022. Induction of brain insulin resistance and Alzheimer's molecular changes by western diet. Int. J. Mol. Sci. 23 (9) https://doi.org/10.3390/ijms23094744.

Montes-Castro, N., Alvarado-Cruz, I., Torres-Sánchez, L., García-Aguiar, I., Barrera-Hernández, A., Escamilla-Núñez, C., Quintanilla-Vega, B., 2019. Prenatal exposure to metals modified DNA methylation and the expression of antioxidant- and DNA defense-related genes in newborns in an urban area. J. Trace Elem. Med. Biol. 55, 110–120. https://doi.org/10.1016/j.jtemb.2019.06.014.

Oishi, Y., Manabe, I., 2020. Organ system crosstalk in cardiometabolic disease in the age of multimorbidity. Front. Cardiovasc. Med. 7, 1–15. https://doi.org/10.3389/fcvm.2020.00064.

Oldham, M.J., Phalen, R.F., Robinson, R.J., Kleinman, M.T., 2004. Performance of a portable whole-body mouse exposure system. Inhal. Toxicol. 16 (9), 657–662. https://doi.org/10.1080/08958370490464670.

Ormazabal, V., Nair, S., Elfeky, O., Aguayo, C., Salomon, C., Zuñiga, F.A., 2018. Association between insulin resistance and the development of cardiovascular disease. Cardiovasc. Diabetol. 17 (1), 1–14. https://doi.org/10.1186/s12933-018-0762-4.

Peterson, M., Shulman, G., 2018. Mechanisms of Insulin Action and Insulin Resistance. Physiol. Rev. 98, 2133–2223. https://doi.org/10.1152/physrev.00063.2017.

Pizoń, T., Rajzer, M., Wojciechowska, W., Wach-Pizoń, M., Drożdż, T., Wróbel, K., Czarnecka, D., 2018. The relationship between plasma renin activity and serum lipid profiles in patients with primary arterial hypertension. JRAAS - J. Renin-Angiotensin-Aldosterone Syst. 19 (4) https://doi.org/10.1177/1470320318810022.

Rojas, J., Bermudez, V., Palmar, J., Sofía Martínez, M., Carlos Olivar, L., Nava, M., Velasco, M., 2018. Review article pancreatic beta cell death. Nov. Potential Mech. Diabetes Ther. https://doi.org/10.1155/2018/9601801.

Stanhope, K., Havel, P., 2008. Endocrine and metabolic effects of consuming beverages sweetened with fructose, glucose, sucrose, or high-fructose corn syrup. Am. J. Clin. Nut. 88, 1733S–1737S. https://doi.org/10.3945/ajcn.2008.25825D.

Vasudha, A., Takashi, K., Evans, R.W., Aya, K., Tomonori, O., Samar, R.E. K., … Sekikawa, A. (2016). Comparison of HOMA-IR, HOMA-β_ and disposition index.pdf, 58(2), 265–271. https://doi.org/10.1007/s00125–014-3414–6.Comparison.

Wallace, T.M., Levy, J.C., Matthews, D.R., 2004. Use and abuse of HOMA modeling. Diabetes Care 27 (6), 1487–1495. https://doi.org/10.2337/diacare.27.6.1487.

WHO. (2022). Retrieved March 8, 2022, from https://www.who.int/news-room/fact-sheets/detail/ambient-(outdoor)-air-quality-and-health#:~:text=Particulate matter (PM),-Definition and principal&text=It affects more people than,substances suspended in the air.

Wolf, K., Popp, A., Schneider, A., Breitner, S., Hampel, R., Rathmann, W., Peters, A., 2016. Association between long-term exposure to air pollution and biomarkers related to insulin resistance, subclinical inflammation, and adipokines. Diabetes 65 (11), 3314–3326. https://doi.org/10.2337/DB15-1567.

Wong, W.-Y., Brown, L., 2014. Induction of metabolic syndrome by excess fructose consumption. In: Turan, B., Dhalla, N.S. (Eds.), *Diabetic Cardiomyopathy: Biochemical and* Molecular M*echanisms* (pp. 41–63). Springer New York, New York, NY https://doi.org/10.1007/978-1-4614-9317-4_3.

Xu, M.X., Ge, C.X., Qin, Y.T., Gu, T.T., Lou, D.S., Li, Q., Tan, J., 2019. Prolonged PM2.5 exposure elevates risk of oxidative stress-driven nonalcoholic fatty liver disease by triggering increase of dyslipidemia. Free Radic. Biol. Med. 130, 542–556. https://doi.org/10.1016/J.FREERADBIOMED.2018.11.016.

Xu, N., Lao, Y., Zhang, Y., Gillespie, D.A., 2012. Akt: A double-edged sword in cell proliferation and genome stability. J. Oncol. https://doi.org/10.1155/2012/951724.

Xu, X., Rao, X., Wang, T., Jiang, S.Y., Ying, Z., Liu, C., Sun, Q. (2012). Effect of co-exposure to nickel and particulate matter on insulin resistance and mitochondrial dysfunction in a mouse model, 1–12.

Zhang, J.S., Gui, Z.H., Zou, Z.Y., Yang, B.Y., Ma, J., Jing, J., Chen, Y.J., 2021. Long-term exposure to ambient air pollution and metabolic syndrome in children and adolescents: A national cross-sectional study in China. Environ. Int. 148, 106383. https://doi.org/10.1016/J.ENVINT.2021.106383.

Zhang, Shuijuan, Zhang, W., Zeng, X., Zhao, W., Wang, Z., Dong, X., Lin, X., 2019. Inhibition of Rac1 activity alleviates PM2.5-induced pulmonary inflammation via the AKT signaling pathway. Toxicol. Lett. 310, 61–69. https://doi.org/10.1016/j.toxlet.2019.04.017.

Zhang, Siqi, Mwiberi, S., Pickford, R., Breitner, S., Huth, C., Koenig, W., Schneider, A., 2021. Longitudinal associations between ambient air pollution and insulin sensitivity: results from the KORA cohort study. Lancet Planet. Health 5 (1), e39–e49. https://doi.org/10.1016/S2542-5196(20)30275-8.

Zheng, L., Dong, H., Zhao, W., Zhang, X., Duan, X., Zhang, H., Sui, G., 2019. An air-liquid interface organ-level lung microfluidics platform for analysis on molecular mechanisms of cytotoxicity induced by cancer-causing fine particles. ACS Sens. 4 (4), 907–917. https://doi.org/10.1021/acssensors.8b01672.